Research Square

Preprints are preliminary reports that have not undergone peer review.
They should not be considered conclusive, used to inform clinical practice,
or referenced by the media as validated information.

Benzyl- and phenyl-disubstituted 1,2,4-oxadiazoles as potent and selective monoamine oxidase B inhibitors: synthesis, SAR and molecular docking studies

Valentina Kotlyarova
Yaroslavl State Pedagogical University named after K.D. Ushinsky
Anton Shetnev
a.shetnev@list.ru

Yaroslavl State Pedagogical University named after K.D. Ushinsky
Valeria Panova
Yaroslavl State Pedagogical University named after K.D. Ushinsky
Sergey Ivanovskiy
Yaroslavl State Pedagogical University named after K.D. Ushinsky
Stephanus Cloete
North-West University
Anél Petzer
North-West University
Jacobus Petzer
North-West University

Research Article

Keywords: oxadiazole, benzyl, disubstitution, monoamine oxidase, MAO, inhibitor, rational design

Posted Date: November 19th, 2026

DOI: https://doi.org/10.21203/rs.3.rs-11563939/v1

License: This work is licensed under a Creative Commons Attribution 4.0 International License.
Read Full License

Additional Declarations: No competing interests reported.

Benzyl- and phenyl-disubstituted 1,2,4-oxadiazoles as potent and selective monoamine oxidase B inhibitors: synthesis, SAR and molecular docking studies

Valentina D. Kotlyarova[1], Anton A. Shetnev[1,2],· Valeria A. Panova[1],· Sergey A. Ivanovskiy[1],· Stephanus J. Cloete[3], Anél Petzer[3], Jacobus P. Petzer[3]

[1] *Pharmaceutical Technology Transfer Center, Yaroslavl State Pedagogical University named after K.D. Ushinsky, 108 Respublikanskaya St., 150000 Yaroslavl, Russia*

[2] *Yaroslavl State Medical University, 5 st. Revolutionary, 150000, Yaroslavl, Russia*

[3] *Pharmaceutical Chemistry and Centre of Excellence for Pharmaceutical Sciences, North-West University, Potchefstroom 2520, South Africa*

Corresponding author:

✉ Anton A. Shetnev

a.shetnev@list.ru

ORCID: 0000-0002-4389-461X (AA Shetnev)

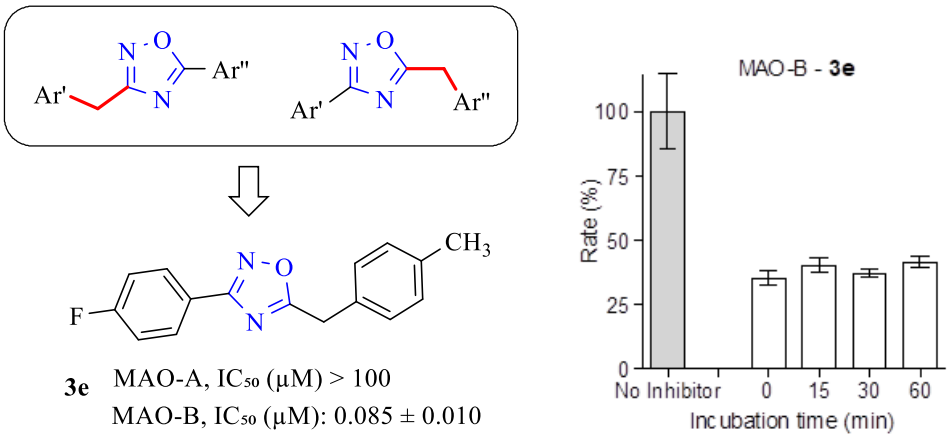
E-Mail Addresses

Valentina D. Kotlyarova	kvd35@mail.ru
Anton A. Shetnev	a.shetnev@list.ru
Valeria A. Panova	lero4ka_aria@mail.ru
Sergey A. Ivanovskiy	main_engine@mail.ru
Stephanus J. Cloete	23496959@mynwu.ac.za
Anél Petzer	anel.petzer@nwu.ac.za
Jacobus P. Petzer	jacques.petzer@nwu.ac.za

Abbreviations:

5-HT, serotonin; AD, Alzheimer's disease; BDNF, brain-derived neurotrophic factor; CDI, carbonyldiimidazole; FAD, flavin adenine dinucleotide; GDNF, glial cell line-derived neurotrophic factor; HRMS, high resolution mass spectrometry; NI, no inhibition; MAO, monoamine oxidase; NMR, nuclear magnetic resonance; PD, Parkinson's disease; PDB, protein data bank; Py, pyridine; ROS, reactive oxygen species; SAR, structure-activity relationship; SD, standard deviation; TCA, TEA, triethylamine; UV, ultraviolet

Graphical abstract



3e MAO-A, IC_{50} (μM) > 100
MAO-B, IC_{50} (μM): 0.085 ± 0.010
New potent reversible inhibitor MAO-B

Abstract

A series of novel 1,2,4-oxadiazole derivatives substituted with both the benzyl and phenyl moieties were investigated as potential selective monoamine oxidase B (MAO-B) inhibitors. The target compounds were synthesized in a two-step, one-pot protocol from arylacetic acids and amidoximes via O-acylamidoxime intermediates, followed by base-catalyzed cyclization; the products were obtained in 65–95% yields without chromatographic purification. All final compounds were fully characterized by ^{1}H and ^{13}C NMR spectroscopy and HRMS, and their purity was confirmed by HPLC-UV (≥95%). The synthesized derivatives were evaluated for their inhibitory activity against human MAO-A and MAO-B. The most active compound, **3e** [3-(4-fluorophenyl)-5-(4-methylbenzyl)-1,2,4-oxadiazole], exhibited an IC_{50} of 0.085 μM against MAO-B with no detectable inhibition of MAO-A at the highest concentration tested (100 μM), thus demonstrating pronounced isoform selectivity. Structure-activity relationship (SAR) analysis revealed that substitution with the benzyl and phenyl on either positions C3 or C5 yielded potent MAO-B inhibitors. It was concluded that the elongated structure of the derivatives was responsible for selective MAO-B inhibition. These results identify disubstitution of 1,2,4-oxadiazole with benzyl and phenyl moieties as a promising strategy for the rational design of potent and selective MAO-B inhibitors, with **3e** representing a valuable lead for further optimization.

Keywords: oxadiazole; benzyl; disubstitution, monoamine oxidase; MAO; inhibitor; rational design.

Introduction

Monoamine oxidases (MAOs) are flavin-dependent (FAD-containing) enzymes located on the outer mitochondrial membrane that catalyze the oxidative deamination of monoamine neurotransmitters such as dopamine, norepinephrine and serotonin (5-HT), as well as exogenous amines such as tyramine and β-phenylethylamine [1,2]. Two isoforms exist in

humans, MAO-A and MAO-B, and are encoded by distinct genes on the X chromosome; they differ in substrate specificity, tissue distribution, and sensitivity to inhibitors [3]. MAO-A primarily metabolizes serotonin and norepinephrine, whereas MAO-B metabolizes β-phenylethylamine and benzylamine, with dopamine and tyramine serving as common substrates [2]. Since the MAO enzymes metabolize neurotransmitter amines in the brain, they have been implicated in the pathogenesis of depression, anxiety disorders, Parkinson's disease (PD), and Alzheimer's disease (AD), making MAO an attractive biological target for drug development [4,5].

Pathological overexpression of MAO-B, which intensifies with age, leads to the excessive production of hydrogen peroxide and reactive oxygen species (ROS), causing mitochondrial damage and neuronal death [5,6]. Studies have shown that MAO-B expression shows an age-related increase in most brains regions, highlighting the neuroprotective potential of selectively inhibiting MAO-B [7]. MAO-B inhibitors reduce ROS production, stimulate the synthesis of neurotrophic factors (GDNF, BDNF), suppress apoptosis, and inhibit α-synuclein aggregation [8,9]. It is worth noting that the clinical value of an MAO inhibitor is determined not only by its affinity for the enzyme but also by its ability to distinguish between these two isoforms, as well as by its safety profile—which depends largely on the reversibility of inhibition and the associated risk of tyramine-induced increase in blood-pressure ("cheese effect") [10]

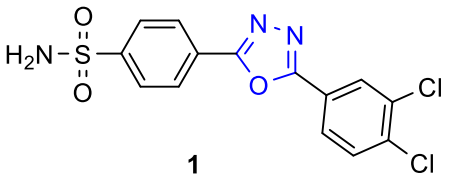
The active sites of MAO-A and MAO-B differ significantly in geometry: the MAO-A cavity is more compact, whereas MAO-B possesses a two-chambered structure comprising an entrance cavity and a substrate cavity [11,12]. X-ray structural data for MAO-A and MAO-B crystals have revealed significant differences between the active sites of the two isoforms: the MAO-B cavity (volume ~700 Å^3) is divided by the Ile199 residue into "substrate" and "entrance" cavities, allowing for the accommodation of larger ligands, whereas the MAO-A cavity (~400 Å^3), due to the substitution of Ile199 for Phe208, cannot undergo such expansion

[13,14]. This implies that the length of the inhibitor directly determines a molecule's ability to occupy both MAO-B cavities and, consequently, its isoform selectivity [13,14]. X-ray crystallography and site-directed mutagenesis have confirmed that the Phe208/Ile199 and Ile335/Tyr326 residues are the primary determinants of the differences in substrate and inhibitor specificity between the isoforms [12,14,15].

Based on the continued interest in MAO inhibitors and their pharmacological applications, the present study set out to design a series of 1,2,4-oxadiazole derivatives as potential selective MAO-B inhibitors [16,17]. We have previously reported several series of oxadiazole compounds with potent and selective MAO-B inhibitory effects. For example, a recent study reported a series of 1,3,4-oxadiazole substituted benzenesulfonamide derivatives that acted as high potency MAO-B inhibitors with all reported compounds exhibiting submicromolar potencies [18]. The most potent derivative (**1**) exhibited an IC_{50} value of 0.0027 μM for the inhibition of MAO-B (Fig. 1). In a second study, 1,2,4-oxadiazole sulfonamide derivatives were investigated, and numerous compounds were found to also potently inhibit MAO-B [19]. One example of a potent MAO-B inhibitor from that study was derivative **2** (IC_{50} = 0.0079 μM). The oxadiazole moiety is thus a valuable scaffold for the design of MAO inhibitors providing two positions as attachment points for substituents. Furthermore, oxadiazole derivatives can be readily synthesized using protocols we had previously reported.

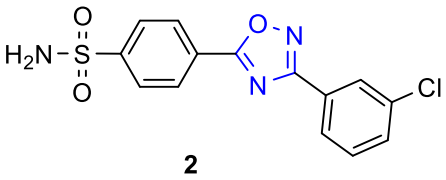
In the present study, we propose novel oxadiazole derivatives containing both a benzyl and phenyl substituent, placed on positions C3 or C5. The derivatives will thus have extended structures that are similar to safinamide, thus increasing the probability that they will possess selectivity for MAO-B over the MAO-A isoform. As noted, longer structures are better suited to binding to the MAO-B active site by spanning both the entrance and substrate cavities [13,14]. The benzyl and phenyl groups were selected as part of an initial exploratory effort to

estimate whether these derivatives will indeed inhibit MAO-B. Halogen and alkyl substituents were placed on these aromatic rings in order to derive structure-activity relationships (SARs). When examining MAO inhibitors that have been reported in literature, a linker group is often present that represents a structural element connecting the key interacting groups to an "anchor" aromatic or heterocyclic moiety [20, 21, 22]. In medicinal chemistry, linker fragments, such as methylene or alkyl bridges, connect pharmacophoric groups while ensuring their optimal spatial orientation within the enzyme's active site. A methylene bridge (–CH_2–) is widely employed in the design of MAO inhibitors as a short, rigid linker connecting an aromatic moiety to a critical interacting group [23,24,25]. The alkyl linker performs several key functions: it regulates the distance between the "anchor" aromatic system and the interacting groups, provides necessary molecular flexibility through sp^3 hybridization, and modulates lipophilicity [23]. In the present study, the oxadiazole derivatives were substituted with a benzyl moiety, which may be viewed as a terminal phenyl linked to the oxadiazole via a methylene linker (Fig. 1). Literature reports several instances where a benzyloxy substituent yield superior MAO-B inhibition compared to the phenoxy-substituted homologue [26, 27]. This suggests the methylene linker present in the benzyl moiety plays a critical role in ensuring the optimal placement and interaction of the inhibitor within the target binding pocket.



1

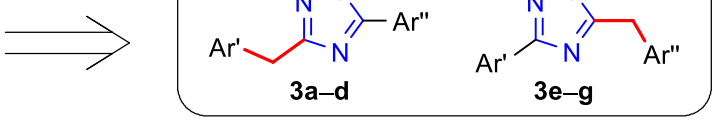
MAO-A: IC_{50} = 46.2 μM
MAO-B: IC_{50} = 0.0027 μM



2

MAO-A: IC_{50} = 95.2 μM
MAO-B: IC_{50} = 0.0079 μM

This study



3a–d **3e–g**

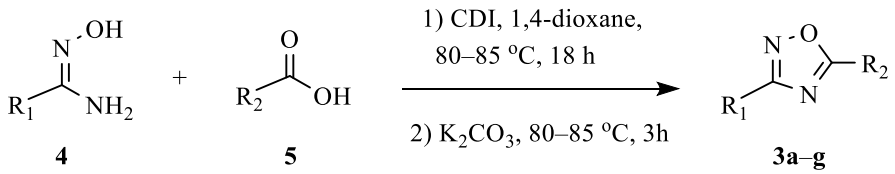
Fig. 1. The approach that was followed for the design of the novel 1,2,4-oxadiazole derivatives of the current study with the methylene linker highlighted.

Results and Discussion

Design, structural rationale and synthesis

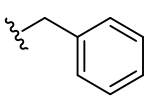
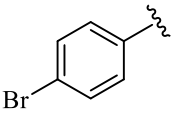
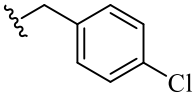
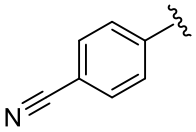
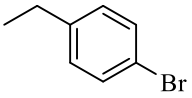
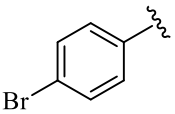
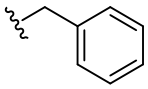
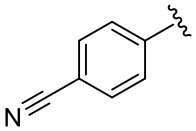
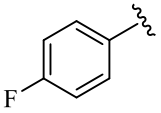
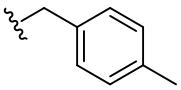
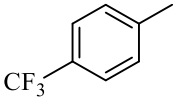
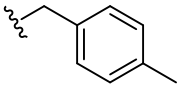
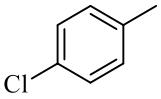
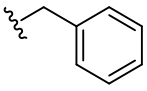
The structure of the target compounds was based on the 1,2,4-oxadiazole moiety, a heterocyclic system previously shown to serve as a bioisosteric replacement for the amide group in tricyclic MAO-A inhibitors [28]; this substitution preserves the biochemical properties of the parent N-arylamides while avoiding their potential toxicity [29,30]. Furthermore, oxadiazole-containing derivatives have been described as MAO-B inhibitors that are effective in Parkinson's disease models, further justifying the choice of this structural core [31].

In the present study, the oxadiazole ring was substituted with the benzyl and phenyl groups yielding a series of disubstituted derivatives (Table 1). Two sub-series were prepared: derivatives with the benzyl moiety on position C3 (**3a–d**) and derivatives with the benzyl moiety on position C5 (**3e–g**). Nitrile-substituted aryl derivatives, in which the terminal moiety was a substituted benzonitrile as well as derivatives, in which the terminal moiety was a halogen- or alkyl-substituted phenyl ring, were included in the study. Both moieties have previously been identified as desirable structural motifs in the design of MAO-B inhibitors, ensuring effective binding to the active site [32, 27]. To synthesize the target structures featuring the oxadiazole core substituted with the benzyl and phenyl moieties on positions C3 and C5 (**3a–g**), this study selected a classical synthetic approach involving the reaction of arylacetic acids and amidoximes, or amidoximes derived from substituted benzyl cyanides (Scheme 1) [33, 34, 35].



Scheme 1. The initial reaction conditions for the synthesis of the 1,2,4-oxadiazole derivatives (**3a–g**).

Table 1. The substitution patterns and yields of the synthesized 1,2,4-oxadiazole derivatives (**3a–g**).

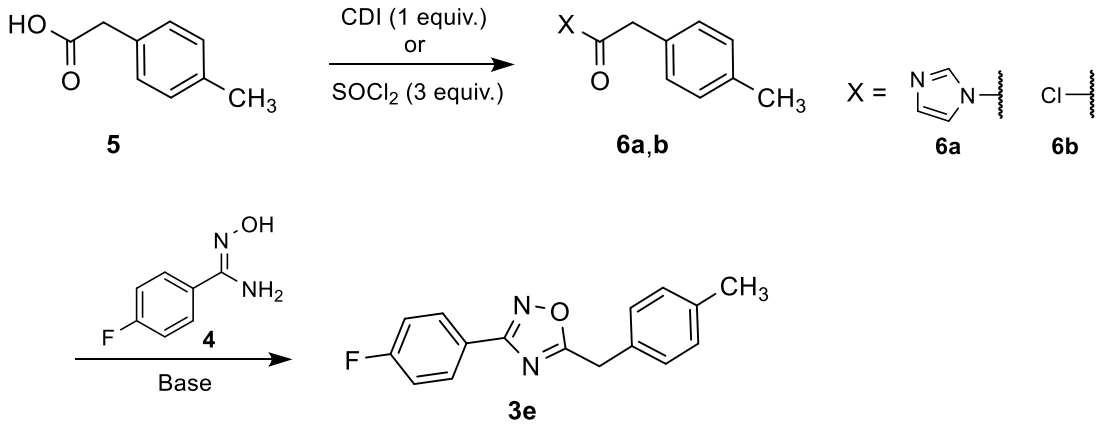
	R^1	R^2	Yield, %
3a			65
3b			78
3c			72
3d			71
3e			84, 95[a]
3f			77
3g			80

[a] Yield of product **3e** under optimized reaction conditions

The reactions were carried out in two stages using a one-pot procedure. Initially, the acid, which was activated with carbonyldiimidazole (CDI) in dioxane, was reacted with an amidoxime to form an O-acylamidoxime. The resulting O-acylamidoxime underwent thermal cyclization without isolation, catalyzed by a weak base (potassium carbonate) according to the method

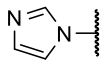
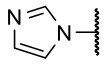
described in literature [33]. This process yielded seven 1,2,4-oxadiazole derivatives with yields ranging from 65 to 84%.

Given that compound **3e** showed the most promise for further pharmaceutical development (see biological evaluation below), we investigated the synthetic conditions and various synthetic routes for this compound in greater detail (Scheme 2). Table 2 presents the results of the optimization of the synthesis conditions for 3-(4-fluorophenyl)-5-(4-methylbenzyl)-1,2,4-oxadiazole (**3e**).



Scheme 2. The optimized reaction conditions for the synthesis of 1,2,4-oxadiazole derivative **3e**.

Table 2. Optimization of the synthetic conditions for 3-(4-fluorophenyl)-5-(4-methylbenzyl)-1,2,4-oxadiazole (**3e**)

Entry	X	Base, equiv.	Solvent	T,℃	Time, h	Yield, %
1[a]		NaOH, 1,1	DMSO	20	18	66
2[a]		K_2CO_3, 1,3	Dioxane	80	18	76-84
3[b]	Cl	TEA, 4	Dioxane	80	18	54 (dark oil)
4[b]	Cl	Py, 4	CH_3CN	80	18	95

[a] The synthesis of 4-methylphenylacetic acid imidazolide (**6a**) was carried out in a one-pot procedure using the reaction solvent en stirring the acid solution with one equiv. of CDI for 30 min.

[b] 4-Methylphenylacetic acid chloride **6b** was prepared separately by treating the starting acid with 3 equiv. of thionyl chloride at 50 °C in the presence of one drop of DMF for 4 h, followed by removal of excess thionyl chloride under vacuum.

Abbreviations: T, temperature; TEA, triethylamine; Py, pyridine.

It was demonstrated that the general synthetic route that was initially selected for oxadiazoles **3a**–**g** did not yield optimal results in terms of product yield and purity when the synthesis of **3e** was reinvestigated. The most optimal conditions for the synthesis of oxadiazole **3e** involved a reaction in pyridine using the acid chloride with heating overnight (18 h). The product obtained under these conditions was isolated by filtration and required no further purification. The procedure will enable simple scale-up from milligram amounts to large quantities. All final products were fully characterized by NMR spectroscopy (^{1}H and ^{13}C) and high-resolution mass spectrometry (HRMS). The obtained spectral data were in full agreement with the proposed structures. In particular, the ^{1}H NMR spectra exhibited a characteristic singlet for the CH_2 protons in the region of δ 4.1–4.4 ppm. On the ^{13}C NMR spectra, the two carbon atoms of the 1,2,4-oxadiazole ring appeared as distinct signals in the range of δ 167–180 ppm, depending on the substituents, which was consistent with literature precedents for such heterocycles [36]. The HRMS data further confirmed the molecular formulas of all target compounds. These observations collectively established the identity and purity of the synthesized derivatives.

MAO-A and MAO-B inhibitory activity

The synthesized compounds were evaluated for their ability to inhibit MAO-A and MAO-B *in vitro*. For these biochemical experiments, the recombinant human MAO enzymes were used

with kynuramine serving as substrate for both isoenzymes [37, 38]. The oxadiazole derivatives were evaluated across a concentration range of 0.003–100 μM, enabling the construction of sigmoidal concentration-response plots from which IC_{50} values were estimated (Fig. 2). The IC_{50} values for the inhibition of the MAOs are presented in Table 3 and show a pronounced and non-uniform SAR, in which the nature of the terminal pharmacophore as well as the substitution pattern contributed to the observed potency and selectivity.

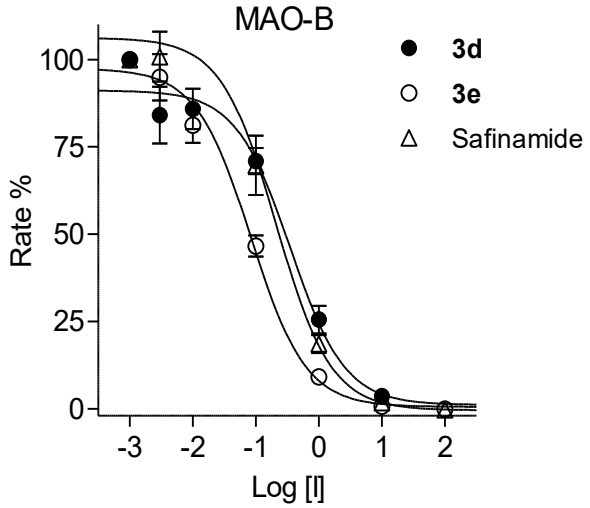
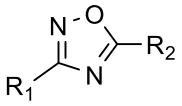
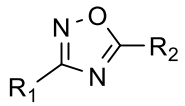


Fig. 2. The sigmoidal concentration-response plots that were constructed for the determination of IC_{50} values for the inhibition of MAO-B by **3d**, **3e** and safinamide.

Table 3. The *in vitro* inhibitory activities of the 1,2,4-oxadiazole derivatives against human MAO-A and MAO-B.

	**R¹**	**R²**	**MAO-A IC₅₀ (μM)[a]**	**MAO-B IC₅₀ (μM)[a]**
3a	benzyl	4-Br-C_6H_4	NI[b]	0.617 ± 0.040
3b	4-Cl-benzyl	4-CN-phenyl	NI[b]	0.783 ± 0.165

	**R¹**	**R²**	**MAO-A IC_{50} (μM)[a]**	**MAO-B IC_{50} (μM)[a]**
3c	4-Br-benzyl	4-Br-C_6H_4	NI[b]	24.4 ± 5.50
3d	benzyl	4-CN-phenyl	NI[b]	0.311 ± 0.099
3e	4-F-C_6H_4	4-CH_3-benzyl	NI[b]	0.085 ± 0.010
3f	4-CF_3-C_6H_4	4-CH_3-benzyl	NI[b]	0.481 ± 0.039
3g	4-Cl-C_6H_4	benzyl	NI[b]	0.951 ± 0.022
Safinamide			NI[b]	0.176± 0.036

[a] Values are means ± standard deviation (SD) of experiments performed in triplicate.

[b] NI, no inhibition observed at the highest concentration tested (100 μM).

Abbreviations: MAO, monoamine oxidase; NI, no inhibition; SD, standard deviation.

The oxadiazole derivatives exhibited considerable variation in MAO-B inhibitory potency. The most active compound in the series, **3e** [3-(4-fluorophenyl)-5-(4-methylbenzyl)-1,2,4-oxadiazole], exhibited an IC_{50} of 0.085 μM against MAO-B, with no detectable MAO-A inhibition. This value was at least threefold more potent than the second most potent compound (**3d**; IC_{50} = 0.311 μM) in the series and identified the 4-methylbenzyl fragment, in combination with a *p*-fluorophenyl substituent on the oxadiazole, as a particularly favourable pharmacophoric combination. It was noteworthy that none of the oxadiazole derivatives inhibited MAO-A at the maximal tested concentration of 100 μM. This aligns with the observation that compounds with longer scaffolds such as safinamide are more prone to inhibit MAO-B by extending across both the substrate and entrance cavities within the active site [13]. In contrast, fused heterocycles (*e.g.*, harmine, methylene blue) are more suited to binding to the MAO-A active site [12, 40].

The inhibition data provided insight into the effect of the different substituents on MAO-B inhibition. These insights could inform the design of future MAO inhibitors: (a) The nitrile-containing derivatives displayed good MAO-B inhibition: **3b** (IC_{50} = 0.783 μM) and **3d** (C_{50} = 0.311 μM). Here the benzyl-substituted derivative was slightly more potent than the chlorobenzyl-substituted compound. (b) Notably, the bromo-substituted derivatives, **3a** and **3c**, showed IC_{50} values of 0.617 and 24.4 μM, respectively. The dramatic difference between these two derivatives, which differed only in the addition of a bromine atom on benzyl fragment, underscored the sensitivity of MAO-B inhibition to the substitution pattern and the spatial arrangement of the halogenated aryl rings. With bromo-substitution on both the benzyl and phenyl rings, the weak MAO-B inhibition potency recorded for **3c** may indicate that the molecular dimensions of the molecule may be too large resulting in unfavorable interactions with the enzyme. (c) Substitution with both halogens (Cl, Br and F) and alkyl groups (CH_3, CF_3) yielded derivatives with submicromolar potencies while all three derivatives that were unsubstituted on one of the terminal phenyl rings (*e.g.*, **3a**, **3d** and **3g**) also displayed good potencies. In fact, except for **3c**, all compounds in the series were potent MAO-B inhibitors. (d) Substitution with the benzyl on either positions C3 (*e.g.*, **3a–b**, **d**) or C5 (*e.g.*, **3e–g**) resulted in potent MAO-B inhibition. This finding indicated that activity mostly depended on the substitution patterns on the benzyl and phenyl moieties rather than their specific positions on the 1,2,4-oxadiazole ring.

In summary, the present series demonstrated that 1,2,4-oxadiazole derivatives bearing benzyl and phenyl substituents can serve as potent and selective MAO-B inhibitors. The most promising compound, **3e**, provides a valuable lead for further optimization, and the systematic variation of the terminal fragment establishes clear SARs that will guide the design of next-generation inhibitors with improved potency and isoform selectivity.

*Mechanism of MAO-B inhibition by **3e***

Since compound **3e** was found to be the most promising MAO-B inhibitor of the series, its mechanism of inhibition was further investigated by constructing a set of Lineweaver-Burk (double-reciprocal) plots [37]. For this purpose, six plots were constructed, one plot in the absence of inhibitor and five plots at concentrations of the inhibitor that bracketed the IC_{50} value (0.021–0.106 μM). For each plot, eight concentrations of kynuramine (15–250 μM) were used. The Lineweaver-Burk plots indicated that compound **3e** was a competitive MAO-B inhibitor since the lines were linear and intersected on the y-axis (Fig. 3). From a secondary plot of the slopes of the Lineweaver-Burk plots versus inhibitor concentration, a K_i value of 0.022 μM was estimated, indicating high potency inhibition of MAO-B by **3e**.

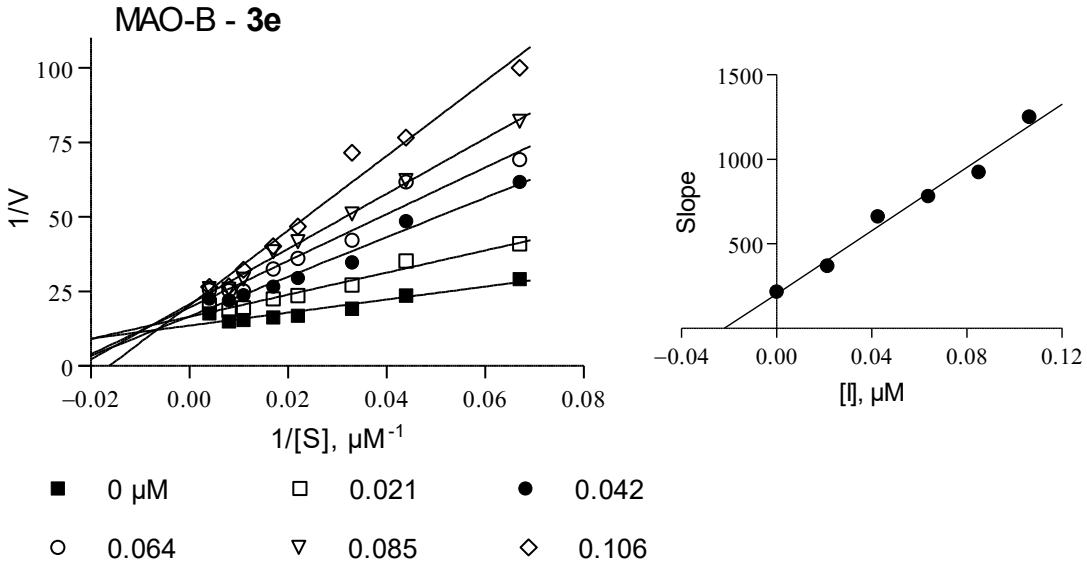


Fig. 3. Lineweaver–Burk plots were generated to assess inhibition of MAO-B. The K_i value (0.022 μM) was estimated by plotting the Lineweaver–Burk slope values against inhibitor concentration.

To investigate the reversibility of MAO-B inhibition by compound **3e**, the time-dependency of inhibition was examined [37]. In this study, MAO-B was incubated with **3e** for different time

periods (0, 15, 30, and 60 min), using **3e** at a concentration of 2 × IC_{50}. Following addition of the substrate, kynuramine, the mixtures were diluted so that the inhibitor concentration corresponded to IC_{50}, and the remaining MAO-B activity was then determined. As shown in Fig. 4, MAO-B activity did not change across the incubation times, indicating that inhibition by **3e** is not time-dependent and is therefore reversible. By comparison, under the same conditions the irreversible MAO-B inhibitor (R)-deprenyl produced a clear, time-dependent decrease in enzyme activity. Collectively, these findings verified that **3e** was a reversible MAO-B inhibitor.

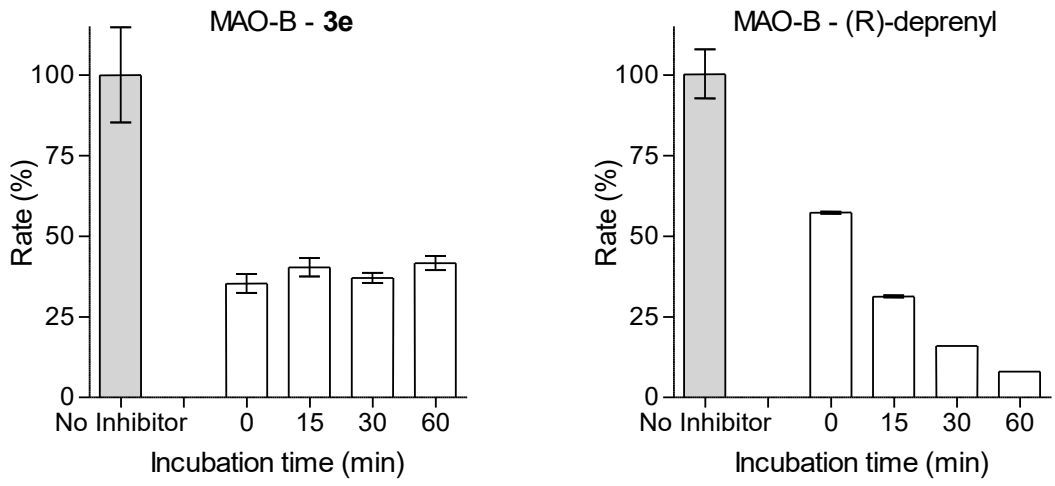


Fig. 4. Time-dependent inhibition of MAO-B. The enzymes were incubated with compound **3e** en the irreversible inhibitor, (R)-deprenyl, for varying time periods, and the remaining enzyme activity was measured.

*Computational docking of **3c** and **3e** into the MAO-B active site*

This study found that 1,2,4-oxadiazole derivative **3e** was a potent MAO-B inhibitor with an IC_{50} value of 0.085 μM. Interestingly, derivative **3c** proved to be a weak inhibitor with an IC_{50} value of 24.4 μM. Derivative **3c** was therefore an exception in this study since all other

compounds exhibited submicromolar inhibition potencies. To investigate the molecular basis for this difference in potency, a molecular docking study was carried out. Molecular modelling was conducted to investigate the potential binding poses and interaction features of derivatives **3c** and **3e** with the active site of MAO-B. The CDOCKER tool in Discovery Studio was used for these simulations, using the crystal structure of human MAO-B (PDB ID: 2V5Z) as the protein model [12, 13]. To validate the docking procedure, the co-crystallized ligand, safinamide, was docked and the root mean square deviation (RMSD) from its position in the crystal structure was measured. The RMSD was found to be 0.44 Å indicating that the protocol was effective at predicting binding poses of ligands to MAO-B.

The predicted binding poses of **3c** and **3e** within the MAO-B active site are displayed in Fig. 5. The two inhibitors exhibited similar binding orientations with the benzyl moiety placed in the substrate cavity of the enzyme while the phenyl substituent extended deep into the entrance cavity, the space beyond the gating residue Ile199, and Tyr326, Leu171 and Phe168, which are the residues that separate the two cavities [11]. The oxadiazole rings of both derivatives formed a single hydrogen bond interaction with residues in the active site: **3e** was hydrogen bonded to the phenolic group of Tyr326 and **3c** to the side chain amide of Gln206. For both derivatives, the oxadiazole rings also formed pi-sulfur interactions with Cys172 while their benzyl rings interacted with Tyr398 by pi-pi stacking. For **3e**, additional pi-pi stacking was observed between the phenyl substituent and Tyr326.

An analysis of the interaction energies for derivatives **3c** and **3e** with MAO-B active site residues was carried out (Fig. 6). As evident from the negative interaction energies, the analysis showed that for both derivatives, residues Leu171, Ile199 and Tyr326 contributed most to ligand stabilization. However, Leu164 and Phe343 formed unfavourable interactions with **3c**,

with a large positive interaction energy (+50.2 kcal/mol) recorded for Leu164 in particular. Derivative **3e** formed an unfavourable interaction with Ile316 (+15.6 kcal/mol), although the interaction energy is significantly smaller (less positive) than between **3c** and Leu164. Due to the unfavourable interaction between **3c** and Leu164, the calculated total interaction energy was 16.2 kcal/mol indicating weak binding to MAO-B (Table 4). In contrast, the total interaction energy for **3e** was –19.1 kcal/mol indicating stronger binding. These results agreed with the in vitro findings that **3e** was a potent MAO-B inhibitor while **3c** displayed weak inhibition. All derivatives and the reference compound, safinamide, also had negative total interaction energies, in agreement with their good potency MAO-B inhibition. This finding suggests that a combination of large size and structural rigidity of **3c** led to an unfavourable interaction with Leu164 resulting in weak MAO-B inhibition.

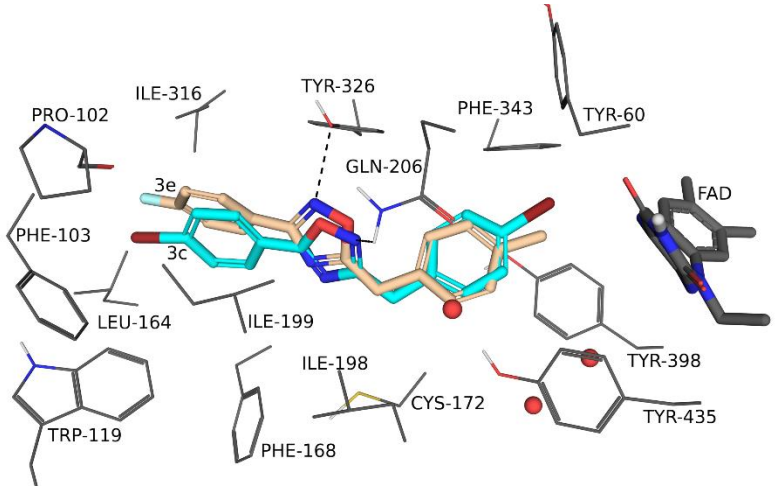


Fig. 5. The binding orientations of **3c** (cyan) and **3e** (wheat) in the MAO-B active site as predicted by molecular docking. The dashed lines indicate hydrogen bonding.

Table 4. The –CDOCKER_ ENERGY and calculated total interaction energy (kcal/mol) of the highest-ranked docked poses of derivatives **3a**–**g**.

	–CDOCKER_ ENERGY[a]	Total interaction energy (kcal/mol)[b]
3a	31.0	–29.8
3b	32.5	–36.4
3c	25.9	16.2
3d	30.8	–21.8
3e	32.0	–19.1
3f	34.4	–38.2
3g	30.5	–27.1
Safinamide	50.4	–45.6

[a] A higher positive value indicates a more thermodynamically favorable overall binding pose.

[b] A more negative value (< 0 kcal/mol) indicates stronger binding.

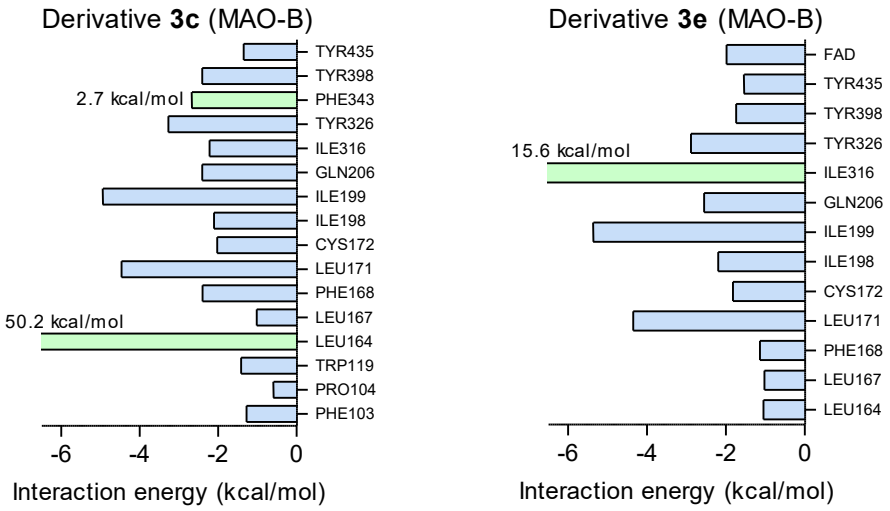


Fig. 6. Estimated per-residue interaction energies for derivatives **3c** and **3e** with MAO-B active-site residues. Only interactions with energies below –1 kcal/mol are displayed. Green bars denote unfavourable interactions corresponding to positive energy values.

Conclusion

In summary, we have discovered novel selective MAO-B inhibitors based on a 1,2,4-oxadiazole core which was substituted with both benzyl and phenyl substituents. A convenient two-step one-pot synthesis provided the target compounds in good yields (65–95%) and high purity, enabling exploration of the SARs of the oxadiazole derivatives. Biological evaluation against human MAO-A and MAO-B revealed interesting SARs, indicating that the nature of the substituent on the benzyl and phenyl rings influenced potency and isoform selectivity. The most active derivative (**3e**) inhibited MAO-B with an IC_{50} of 0.085 μM and showed no detectable MAO-A inhibition at 100 μM, making it a selective inhibitor. The combination of a 4-methylbenzyl fragment with a *p*-fluorophenyl substituent on the oxadiazole ring was identified as a particularly favourable pharmacophoric pairing. Except for **3c**, all derivatives that were studied displayed submicromolar MAO-B inhibition (IC_{50} = 0.085–0.951 μM). Interestingly, two bromo-substituted derivatives **3a** and **3c** differed dramatically in potency (IC_{50} = 0.617 μM vs. 24.4 μM), underscoring the sensitivity of MAO-B inhibition to the spatial arrangement of halogen substituents on the terminal aryl rings.

Taken together, the 1,2,4-oxadiazole derivatives substituted with both benzyl and phenyl moieties represent promising and readily accessible compounds for the development of next-generation MAO-B inhibitors. Further optimization of **3e**, including variation of the linker length and substitution of the terminal aryl rings, is currently underway in our laboratories.

Materials and methods

Chemicals and instrumentation

Reagents and solvents were obtained from commercial sources (Acros, Merck) and were used without additional purification. All reactions were performed in an open flask and reactions were monitored by analytical thin layer chromatography (TLC) using Macherey-Nagel TLC sheets (Polygram® Sil G/UV254). Visualization of the developed TLC sheets was performed

by fluorescence quenching at 254 nm. ^{1}H and ^{13}C NMR spectra were recorded on a Bruker AVANCE DPX 400 spectrometer at 400 MHz for ^{1}H and 100 MHz for ^{13}C, respectively. Chemical shifts (δ) are given in parts per million (ppm) with reference to solvent residues in DMSO-d_6 (2.50 for proton and 39.52 for carbon) and coupling constants (*J)* are reported in hertz (Hz). Multiplicities are abbreviated as follows: s = singlet, d = doublet, t = triplet, q = quartet, m = multiplet, br = broad. Melting points were determined on Electrothermal IA 9300 series digital melting point apparatus. Mass spectra were recorded on microTOF spectrometers (ESI mode).

*General procedure for the synthesis of the 1,2,4-oxadiazole derivatives (**3a**–**g**)*

To a stirred suspension of a carboxylic acid (1.1 equiv.) in 1,4-dioxane (15 mL per gram of carboxylic acid) was added CDI (1.1 equiv.). The reaction mixture was stirred at room temperature for 1 h, and an amidoxime (1.0 equiv.) was added. The resulting mixture was stirred at 80–85 ºC for 18 h. Next, powdered K_2CO_3 (1.3 equiv.) was rapidly added and the reaction mixture was stirred at 80–85 ºC for 3 h. The reaction mixture was then concentrated under vacuum, and the residue was diluted with cold water (30 mL). The resulting precipitate was filtered, washed with cold water (25 mL), and air-dried at a temperature of 50 °C [33].

*3-Benzyl-5-(4-bromophenyl)-1,2,4-oxadiazole (**3a**).*

White powder; 65% yield; mp 110–112 °C. ^{1}H NMR (400 MHz, DMSO-d_6) δ 7.97 (d, J = 8.6 Hz, 2H), 7.79 (d, J = 8.6 Hz, 2H), 7.39 – 7.21 (m, 5H), 4.16 (s, 2H). ^{13}C NMR (101 MHz, DMSO-d_6) δ 175.13, 170.71, 136.34, 133.20, 130.29, 129.52, 129.15, 127.62, 127.49, 123.51, 32.27. HRMS (ESI), m/z: $[M+H]^+$ calcd for $C_{15}H_{12}BrN_2O$ 315.0128; found 315.0130.

*4-(3-(4-Chlorobenzyl)-1,2,4-oxadiazol-5-yl)benzonitrile (**3b**).*

White powder; 78% yield; mp 137–138 °C. ^{1}H NMR (400 MHz, DMSO-d_6) δ 8.21 (d, J = 8.1 Hz, 2H), 8.06 (d, J = 8.4 Hz, 2H), 7.38 (s, 4H), 4.21 (s, 2H). ^{13}C NMR (101 MHz, DMSO) δ

174.49, 170.66, 135.21, 134.06, 132.42, 131.55, 130.26, 129.20, 127.79, 118.57, 115.94, 31.33. HRMS (ESI), m/z: $[M+H]^+$ calcd for $C_{16}H_{11}ClN_3O$ 296.0585; found 296.0585.

*3-(4-Bromobenzyl)-5-(4-bromophenyl)-1,2,4-oxadiazole (**3c**).*

White powder; 72% yield; mp 136–137 °C. ^{1}H NMR (400 MHz, DMSO-d_6) δ 7.98 (d, J = 8.2 Hz, 2H), 7.80 (d, J = 8.7 Hz, 2H), 7.52 (d, J = 8.0 Hz, 2H), 7.32 (d, J = 8.1 Hz, 2H), 4.17 (s, 2H). ^{13}C NMR (101 MHz, DMSO-d_6) δ 175.25, 170.37, 135.79, 133.25, 132.10, 131.81, 130.34, 127.69, 123.46, 120.84, 31.63. HRMS (ESI), m/z: $[M+H]^+$ calcd for $C_{15}H_{11}Br_2N_2O$ 392.9233; found 392.9235.

*4-(3-Benzyl-1,2,4-oxadiazol-5-yl)benzonitrile (**3d**)* [39].

White powder; 71% yield; mp 117–118 °C. ^{1}H NMR (400 MHz, DMSO-d_6) δ 8.21 (d, J = 8.3 Hz, 2H), 8.06 (d, J = 8.5 Hz, 2H), 7.37 – 7.22 (m, 5H), 4.20 (s, 2H). ^{13}C NMR (101 MHz, DMSO) δ 174.41, 170.93, 136.20, 134.04, 129.63, 129.28, 129.18, 127.82, 127.63, 118.58, 115.90, 32.03. HRMS (ESI), m/z: $[M+H]^+$ calcd for $C_{16}H_{12}N_3O$ 262.0975; found 262.0976.

*5-(4-Methylbenzyl)-3-(4-(trifluoromethyl)phenyl)-1,2,4-oxadiazole (**3f**).*

White powder; 77% yield; mp 73–74 °C. ^{1}H NMR (400 MHz, DMSO-d_6) δ 8.19 (d, J = 8.0 Hz, 2H), 7.92 (d, J = 8.0 Hz, 2H), 7.28 (d, J = 7.7 Hz, 2H), 7.18 (d, J = 7.4 Hz, 2H), 4.41 (s, 2H), 2.28 (s, 3H). ^{13}C NMR (101 MHz, DMSO) δ 180.31, 167.45, 137.26, 134.11, 132.18, 131.85, 131.49, 130.68, 130.00, 129.65, 128.52, 126.89, 126.85, 125.84, 123.13, 32.27, 21.29. HRMS (ESI), m/z: $[M+H]^+$ calcd for $C_{17}H_{14}F_3N_2O$ 319.1053; found 319.1053.

*5-Benzyl-3-(4-chlorophenyl)-1,2,4-oxadiazole (**3g**).*

White powder; 80% yield; mp 97–98 °C. ^{1}H NMR (400 MHz, DMSO-d_6) δ 7.99 (d, J = 8.3 Hz, 2H), 7.62 (d, J = 8.4 Hz, 2H), 7.42 – 7.28 (m, 5H), 4.44 (s, 2H). ^{13}C NMR (101 MHz, DMSO) δ 179.80, 167.65, 136.96, 134.64, 130.07, 129.75, 129.62, 129.46, 128.06, 125.67, 32.66. HRMS (ESI), m/z: $[M+H]^+$ calcd for $C_{15}H_{12}ClN_2O$ 271.0633; found 271.0635.

*Scalable procedure for the synthesis of the 1,2,4-oxadiazole derivatives (**3e**)*

To a stirred solution of the amidoxime (1.0 equiv.) in CH_3CN (13 mL per gram of amidoxime) was added pyridine (1.25 equiv.). The reaction mixture was cooled to 0 °C, and the chloroanhydride of 4-methylphenylacetic acid was added dropwise at 0–5 °C. The ice bath was removed and the resulting mixture was stirred at room temperature for 1 h and then heated at 85–90 °C for 18 h. The solvent was removed under vacuum, and the residue was diluted with 1% HCl (15 mL) per gram of starting amidoxime solution, and the resulting precipitate was collected by filtration, washed with cold water (25 mL per gram of starting amidoxime), and air-dried at 50 °C. The product obtained under these conditions required no further purification.

*3-(4-Fluorophenyl)-5-(4-methylbenzyl)-1,2,4-oxadiazole (**3e**).*

White powder; 95% yield; mp 80–81 °C. ^{1}H NMR (400 MHz, DMSO-d_6) δ 8.03 (dd, J = 9.0, 5.4 Hz, 2H), 7.38 (t, J = 8.9 Hz, 2H), 7.27 (d, J = 7.8 Hz, 2H), 7.17 (d, J = 7.8 Hz, 2H), 4.37 (s, 2H), 2.28 (s, 3H). ^{13}C NMR (101 MHz, DMSO) δ 179.83, 167.60, 165.83, 163.35, 137.21, 131.61, 130.24, 130.15, 129.99, 129.60, 123.41, 117.17, 116.95, 32.25, 31.99, 21.30. HRMS (ESI), m/z: $[M+H]^+$ calcd for $C_{16}H_{14}FN_2O$ 269.1085; found 269.1086

MAO inhibition studies

The inhibitory effects of the synthesized compounds were assessed using commercially sourced recombinant human MAO-A and MAO-B (Merck) according to an established procedure [37, 38]. Kynuramine was used as the substrate for both MAO isoforms and was oxidized to produce the fluorescent metabolite 4-hydroxyquinoline. Formation of 4-hydroxyquinoline was quantified by fluorescence spectrometry (λ_{ex} = 310 nm; λ_{em} = 400 nm). In this assay, MAO-catalyzed oxidation of kynuramine was measured in the presence of varying inhibitor concentrations (0.003–100 μM) as well as under inhibitor-free conditions. The data were then used to construct sigmoidal curves of reaction rate versus the logarithm of inhibitor concentration (log[I]), from which IC_{50} values were calculated and reported as the mean ± standard deviation (SD) of three determinations.

Construction of Lineweaver-Burk (double-reciprocal) plots

To establish the mode of inhibition, Lineweaver–Burk plots were constructed [37]. In total, six plots were generated for compound **3e**: five at inhibitor concentrations covering the IC_{50} range (0.021–0.106 μM) and one control plot with no inhibitor. Each line was based on data collected at eight kynuramine concentrations (15–250 μM). The slopes from the Lineweaver–Burk plots were subsequently plotted versus inhibitor concentration, and the K_i was determined from the x-intercept of this secondary plot (K_i = –x-intercept).

Determination of the reversibility of inhibition

The reversibility of inhibition was evaluated by preincubating MAO-B with compound **3e** at twofold its experimentally determined IC_{50} for 0-, 15-, 30-, or 60-min. Reactions were then initiated by adding an equal volume of kynuramine, yielding a final inhibitor concentration corresponding to its IC_{50}. Incubations proceeded for a further 20 min at room temperature, after which formation of 4-hydroxyquinoline (as an indicator of residual MAO catalytic activity) was measured as previously reported [37]. In parallel, control experiments were conducted with the irreversible inhibitor (R)-deprenyl.

Procedure for molecular docking

Molecular docking was performed following the methodology described in the literature [19]. All simulations were conducted using the Discovery Studio 3.1 life sciences software package, employing the X-ray crystal structure of MAO-B complexed with safinamide (PDB ID: 2V5Z) as the protein model [13].

Supplementary information

The online version of supplementary materials available at https://doi.org/10.1007/xxxxxx-xxx-xxxxx-x.

Funding

This study was supported by the Russian Science Foundation (project number 25-23-00728). This work was financially supported by the National Research Foundation of South Africa [Grant specific unique reference numbers (UID) 137997]. The Grantholders acknowledge that opinions, findings and conclusions or recommendations expressed in any publication generated by the NRF supported research are that of the authors, and that the NRF accepts no liability whatsoever in this regard.

Compliance with ethical standards

Conflict of interest

The authors declare no competing interests.

Publisher's note

Springer Nature remains neutral with regard to jurisdictional claims in published maps and institutional affiliations.

References

[1] Hong R, Li X. Discovery of monoamine oxidase inhibitors by medicinal chemistry approaches. Med Chem Comm. 2019;10(1):10-25. https://doi.org/10.1039/c8md00446c.

[2] Youdim MB, Edmondson D, Tipton KF. The therapeutic potential of monoamine oxidase inhibitors. Nat Rev Neurosci. 2006;7(4):295-309. https://doi.org/10.1038/nrn1883.

[3] Shih JC, Chen K, Ridd MJ. Monoamine oxidase: from genes to behavior. Annu Rev Neurosci. 1999;22:197-217. https://doi.org/10.1146/annurev.neuro.22.1.197.

[4] Ramsay RR. Monoamine oxidases: The biochemistry of the proteins as targets in medicinal chemistry and drug discovery. Curr Top Med Chem. 2012;12(20):2189-209. DOI: https://doi.org/10.2174/156802612805219978.

[5] Youdim MBH, Bakhle YS. Monoamine oxidase: isoforms and inhibitors in Parkinson's disease and depressive illness. Brit J Pharmacol. 2006;147:287-96. https://doi.org/10.1038/sj.bjp.0706464.

[6] Edmondson DE. Hydrogen peroxide produced by mitochondrial monoamine oxidase catalysis: biological implications. Curr Pharm Des. 2014;20(2):155-60. https://doi.org/10.2174/13816128113190990406.

[7] Fowler JS, Volkow ND, Wang GJ, Logan J, Pappas N, Shea C, MacGregor R. Age-related increases in brain monoamine oxidase B in living healthy human subjects. Neurobiol Aging. 1997;18(4):431-5. https://doi.org/10.1016/s0197-4580(97)00037-7.

[8] Alborghetti M, Bianchini E, De Carolis L, Galli S, Pontieri FE, Rinaldi D. Type-B monoamine oxidase inhibitors in neurological diseases: clinical applications based on preclinical findings. Neural Regen Res. 2024;19(1):16-21. https://doi.org/10.4103/1673-5374.375299.

[9] Robakis D, Fahn S. Defining the role of the monoamine oxidase-B inhibitors for Parkinson's disease. CNS Drugs. 2015;29(6):433-41. https://doi.org/10.1007/s40263-015-0249-8.

[10] Finberg JP, Gillman K. Selective inhibitors of monoamine oxidase type B and the "cheese effect". Int Rev Neurobiol. 2011;100:169-90. https://doi.org/10.1016/B978-0-12-386467-3.00009-1.

[11] Binda C, Newton-Vinson P, Hubalek F, Edmondson DE, Mattevi A. Structure of human monoamine oxidase B, a drug target for the treatment of neurological disorders. Nat Struct Biol. 2002;9(1):22-6. https://doi.org/10.1038/nsb732.

[12] Son SY, Ma J, Kondou Y, Yoshimura M, Yamashita E, Tsukihara T. Structure of human monoamine oxidase A at 2.2-A resolution: the control of opening the entry for substrates/inhibitors. Proc Natl Acad Sci USA. 2008;105(15):5739-44. https://doi.org/10.1073/pnas.0710626105.

[13] Binda C, Wang J, Pisani L, Caccia C, Carotti A, Salvati P, Edmondson DE, Mattevi A. Structures of human monoamine oxidase B complexes with selective noncovalent inhibitors:

safinamide and coumarin analogs. J Med Chem. 2007;50(23):5848-52. https://doi.org/10.1021/jm070677y.

[14] Hubálek F, Binda C, Khalil A, Li M, Mattevi A, Castagnoli N, Edmondson DE. Demonstration of isoleucine 199 as a structural determinant for the selective inhibition of human monoamine oxidase B by specific reversible inhibitors. J Biol Chem. 2005;280(16):15761-6. https://doi.org/10.1074/jbc.M500949200.

[15] Geha RM, Rebrin I, Chen K, Shih JC. Substrate and inhibitor specificities for human monoamine oxidase A and B are influenced by a single amino acid. J Biol Chem. 2001;276(13):9877-82. https://doi.org/10.1074/jbc.M006972200.

[16] Guglielmi P, Carradori S, D'Agostino I, Campestre C, Petzer JP. An updated patent review on monoamine oxidase (MAO) inhibitors. Expert Opin Ther Pat. 2022;32(8):849-83. https://doi.org/10.1080/13543776.2022.2083501.

[17] Shaldam MA, Carradori S, Balaha M, Guglielmi P, Diomede F, D'Agostino I, Tawfik HO. Patents involving monoamine oxidase (MAO): A comprehensive update (2022-2025) on its inhibitors and applications. Expert Opin Ther Pat. 2026;36(4):363-87. https://doi.org/10.1080/13543776.2026.2633345.

[18] Shetnev A, Shlenev R, Efimova J, Ivanovskii S, Tarasov A, Petzer A, Petzer JP. 1,3,4-Oxadiazol-2-ylbenzenesulfonamides as privileged structures for the inhibition of monoamine oxidase B. Bioorg Med Chem Lett. 2019;29(21):126677. https://doi.org/10.1016/j.bmcl.2019.126677.

[19] Shetnev AA, Gasilina OA, Baykov SV, Turmanov R, Appazov N, Zhapparbergenov R, Togyzbayeva N, Korsakov MK, Cloete SJ, Petzer A, Petzer JP. Synthesis of 1,2,4-oxadiazole sulfonamide derivatives and their biological investigation as monoamine oxidase inhibitors. Molecules. 2026;31(18):3326. https://doi.org/10.3390/molecules31183326.

[20] Gnerre C, Catto M, Leonetti F, Weber P, Carrupt PA, Altomare C, Carotti A, Testa B. Inhibition of monoamine oxidases by functionalized coumarin derivatives: Biological activities, QSARs, and 3D-QSARs. J Med Chem. 2000;43(25):4747-58. https://doi.org/10.1021/jm001028o.

[21] Stear C, Petzer A, Crous C, Petzer JP. Indazole derivatives as novel inhibitors of monoamine oxidase and D-amino acid oxidase. Med Chem Res. 2024;33(1):164-76. https://doi.org/10.1007/s00044-023-03176-x.

[22] Strydom B, Malan SF, Castagnoli N, Bergh JJ, Petzer JP. Inhibition of monoamine oxidase by 8-benzyloxycaffeine analogues. Bioorg Med Chem. 2010;18(3):1018-28. https://doi.org/10.1016/j.bmc.2009.12.064.

[23] Bekircan O, Danış Ö, Şahin ME, Çetin M. Monoamine oxidase A and B inhibitory activities of 3,5-diphenyl-1,2,4-triazole substituted [1,2,4]triazolo[3,4-b][1,3,4]thiadiazole derivatives. Bioorg Chem. 2022;118:105493. https://doi.org/ 10.1016/j.bioorg.2021.105493.

[24] Çevik UA, Osmaniye D, Saglik BN, Levent S, Çavusoglu BK, Özkay Y, Kaplancikli ZA. Synthesis and evaluation of new pyrazoline-thiazole derivatives as monoamine oxidase inhibitors. J Heterocyclic Chem. 2019;56(11):3000-7. https://doi.org/10.1002/jhet.3694.

[25] Tripathi RKP, Ayyannan SR. Design, synthesis, and evaluation of 2-amino-6-nitrobenzothiazole-derived hydrazones as MAO inhibitors: role of the methylene spacer group. ChemMedChem 2016;11(14):1551-67. https://doi.org/10.1002/cmdc.201600202.

[26] Manley-King CI, Bergh JJ, Petzer JP. Inhibition of monoamine oxidase by selected C5- and C6-substituted isatin analogues. Bioorg Med Chem. 2011;19(1):261-74. https://doi.org/10.1016/j.bmc.2010.11.028.

[27] Manley-King CI, Bergh JJ, Petzer JP. Monoamine oxidase inhibition by C4-substituted phthalonitriles. Bioorg Chem. 2012;40(1):114-24. https://doi.org/10.1016/j.bioorg.2011.10.003.

[28] Shetnev A, Osipyan A, Baykov S, Sapegin A, Chirkova Z, Korsakov M, Petzer A, Engelbrecht I, Petzer JP. Novel monoamine oxidase inhibitors based on the privileged 2-imidazoline molecular framework. Bioorg Med Chem Lett. 2019;29(1):40-6. https://doi.org/10.1016/j.bmcl.2018.11.018.

[29] Camci M, Karali N. Bioisosterism: 1,2,4-oxadiazole rings. Chem Med Chem. 2023;18(9):e202200638. https://doi.org/10.1002/cmdc.202200638.

[30] Harfenist M, Heuser DJ, Joyner CT, Batchelor JF, White HL. Selective inhibitors of monoamine oxidase. 3. Structure-activity relationship of tricyclics bearing imidazoline,

oxadiazole, or tetrazole groups. J Med Chem. 1996;39(9):1857-63. https://doi.org/10.1021/jm950595m.

[31] Karabelyov V, Angelova VT, Sharkov M, Mihaylova R, Popov G, Pencheva T, Manov V, Dangalov M, Todorova N, Kondeva-Burdina M. In vitro/in vivo effects of some new 2,5-disubstituted 1,3,4-oxadiazole and hydrazone analogues targeting Parkinson's disease. J Mol Struct. 2023;1288:135755. https://doi.org/10.1016/j.molstruc.2023.135755.

[32] Chirkova ZV, Kabanova MV, Filimonov SI, Abramov IG, Petzer A, Petzer JP, Firgang SI, Suponitsky KY. Inhibition of monoamine oxidase by indole-5,6-dicarbonitrile derivatives. Bioorg Med Chem Lett. 2015;25(6):1206-11. https://doi.org/10.1016/j.bmcl.2015.01.061

[33] Rajagopalan P. Dipolar addition reactions of nitrile oxides. VII. A new general method of synthesis of 3,5-disubstituted 1,2,4-oxadiazoles. Tetrahedron Lett. 1969;10(5):311-2. https://doi.org/https://doi.org/10.1016/S0040-4039(01)87679-6.

[34] Basu S, Prasad UV, Barawkar DA, De S, Palle VP, Menon S, Patel M, Thorat S, Singh UP, Das Sarma K, Waman Y, Niranjan S, Pathade V, Gaur A, Reddy S, Ansari S. Discovery of novel and potent heterocyclic carboxylic acid derivatives as protein tyrosine phosphatase 1B inhibitors. Bioorg Med Chem Lett. 2012;22(8):2843-9. https://doi.org/10.1016/j.bmcl.2012.02.070.

[35] Porcheddu A, Cadoni R, De Luca L. A fast and efficient one-pot microwave assisted synthesis of variously di-substituted 1,2,4-oxadiazoles. Org Biomol Chem. 2011;9(21):7539-46. https://doi.org/10.1039/c1ob06055d.

[36] Baykov S, Sharonova T, Osipyan A, Rozhkoy S, Shetnev A, Smirnov A. A convenient and mild method for 1,2,4-oxadiazole preparation: cyclodehydration of O-acylamidoximes in the superbase system MOH/DMSO. Tetrahedron Lett. 2016;57(26):2898-900. https://doi.org/10.1016/j.tetlet.2016.05.071.

[37] Mashishi MG, Petzer JP, Crous C, Petzer A. The monoamine oxidase inhibition properties of indazole derivatives. Results Chem. 2026;27:103461. https://doi.org/10.1016/j.rechem.2026.103461.

[38] Weissbach H, Smith TE, Daly JW, Witkop B, Udenfriend S. A rapid spectrophotometric assay of mono-amine oxidase based on the rate of disappearance of kynuramine. J Biol Chem. 1960;235:1160-3. https://doi.org/10.1016/S0021-9258(18)69497-9.

[39] Jenkins H, Kitt M, Pearlman R, Serafini T, Thorsett E. Pharmaceutical compositions and methods for treating hyperuricemia and related disorders. U.S. Patent Application US20100160351A1, 2009.

[40] Myburg T, Petzer A, Petzer JP. The inhibition of monoamine oxidase by harmine derivatives. Results Chem. 2022;4:100607. https://doi.org/10.1016/j.rechem.2022.100607.

Supplementary Files

This is a list of supplementary files associated with this preprint. Click to download.

- MethylenesPaperSuppl4.docx